ARTICLE NO. 80-4001

G80-004

Dual-Spin Spacecraft Dynamics During Platform Spinup

70004
70030

G.J. Adams*
Hughes Aircraft Company, Space and Communications Group, Los Angeles, Calif.

Design of the attitude stabilization system of a dual-spin spacecraft is based primarily on proper management of internal energy dissipation with the platform despun. If the platform is rotating, the dynamic response is determined by platform dynamic imbalance and rotor transverse inertia symmetry in addition to energy dissipation effects. The rotating platform case is important as a temporary condition from which it is desired to recover. This paper gives a heuristic description of the vehicle dynamics for roll/pitch ratios above and below unity, a summary of in-order experience with the TACSAT and DSCS-II satellites, and a description of some of the design features and operational procedures utilized on current dual-spin spacecraft to ensure recovery from various failure mode conditions.

Introduction

A NONUNIFORM payload platform mass distribution for a dual-spin satellite leads to the possibility that anamalous dynamic states may occur if despin control is temporarily absent, allowing the platform to rotate. This is a relatively new problem area and one of considerable practical importance as demonstrated in-orbit in recent years. Investigation of large-angle dual-spin dynamics for a range of inertia parameters reveals several dynamic response characteristics associated with an unbalanced platform and rotor transverse inertia asymmetry. Therefore, consideration of platform spinup dynamics is a key part of the overall spacecraft design process.

A number of papers have appeared in the literature concerning the large-angle dynamics of spinning satellites. References 1 and 2 represent some of the earliest work in this area, but consideration was limited to the idealized case of a symmetric rotor. References 3 and 4 address flat spin recovery using various combinations of thrusters for a single-body spinner that must rely on active nutation control in a transfer orbit phase. Perturbation methods are applied to obtain an approximate analytical solution for the recovery dynamics of a dual-spin satellite with a symmetric rotor in Ref. 5, with the principal emphasis on the mathematics involved and on convergence to a suitable small final nutation angle. References 6 and 7 deal with reorienting a momentum bias body-stabilized satellite by spinup of the internal momentum wheel, a maneuver similar to flat spin recovery in a dynamic sense and a case in which the rotor body can be properly assumed to be symmetric. Reference 8 is the first published treatment of large-angle dynamics for an oblate (roll/pitch inertia ratio > 1) dual-spin satellite with both platform dynamic unbalance and rotor transverse inertia asymmetry. Reference 9 provides an analysis and geometric interpretation of the resonance trap identified in Ref. 8 in terms of integrals of averaged equations. Reference 10 and related internal documents consider vehicles with roll/pitch ratio less than unity and with realistic treatment of various mass asymmetries. This paper discusses a heuristic model of large-angle dynamic behavior for a range of inertia parameters, briefly reviews the DSCS-II and TACSAT in-orbit experiences, and identifies some of the design features for current and future dual-spin satellites that ensure recovery from temporary platform spinup.

Received March 27, 1978; revision received June 18, 1979.

Index categories: Spacecraft Dynamics and Control; Spacecraft Systems.

*Project Manager, Defense Systems Division. Member AIAA.

Description of Model

The essential dynamic properties of interest can be demonstrated with the simplified model in Fig. 1. The platform, which has its center of mass on the bearing axis, has a crossproduct of inertia I_{cp} and a transverse inertia difference ΔI_p. Axes x_p, y_p, and z_p form an orthogonal triad located at the platform center of mass, with the z_p axis coincident with the bearing axis. The x_r, y_r, z_r set is defined similarly for the rotor and is rotated relative to the platform coordinates by a relative angle $\emptyset$ about the z_p axis in a positive counter-clockwise sense. The rotor also has a transverse inertia difference ΔI_r. The x, y, and z coordinates are located at the system center of mass and are fixed relative to the platform.

Figure 2 depicts the orientation of the x, y, z coordinates relative to inertial coordinates. x_i, y_i, z_i are fixed inertial coordinates with z_i along the spacecraft angular momentum vector. 1, 2, 3 is a rotating set having the propety that 2 is along the spacecraft transverse angular velocity vector, and 3 is coincident with z. 1, 2, 3 is related to x_i, y_i, z_i by

$$\begin{bmatrix} 1 \\ 2 \\ 3 \end{bmatrix} = \begin{bmatrix} 1 & 0 & 0 \\ 0 & \cos\theta & \sin\theta \\ 0 & -\sin\theta & \cos\theta \end{bmatrix} \begin{bmatrix} \cos\psi & \sin\psi & 0 \\ -\sin\psi & \cos\psi & 0 \\ 0 & 0 & 1 \end{bmatrix} \begin{bmatrix} x_i \\ y_i \\ z_i \end{bmatrix} \tag{1}$$

and x, y, z is related to 1, 2, 3 by

$$\begin{bmatrix} x \\ y \\ z \end{bmatrix} = \begin{bmatrix} \cos\beta_p & \sin\beta_p & 0 \\ -\sin\beta_p & \cos\beta_p & 0 \\ 0 & 0 & 1 \end{bmatrix} \begin{bmatrix} 1 \\ 2 \\ 3 \end{bmatrix} \tag{2}$$

θ is the half-angle of coning of the z-axis about the angular momentum vector direction z_i. ψ is the phase angle of coning, and β_p locates the x axis, fixed in platform reference coordinates, relative to the transverse angular velocity associated with coning.

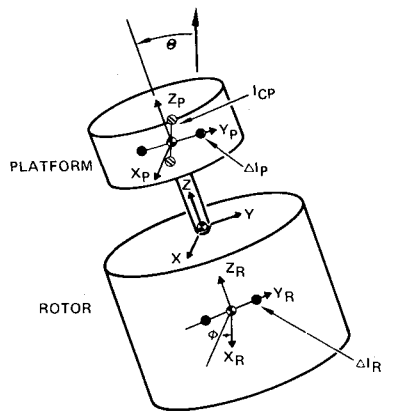

Fig. 1 Vehicle coordinates and mass asymmetries.

$$\beta_r = \beta_p + \emptyset \tag{3}$$

similarly locates the rotor x_r axis relative to the 1,2,3 coordinates.

The system angular momentum is

$$\bar{H} = \bar{\bar{I}}^p \cdot \bar{\omega}^p + \bar{\bar{I}}^r \cdot \bar{\omega}^r = \bar{H}_p + \bar{H}_r \tag{4}$$

where $\bar{\bar{I}}^p$, $\bar{\bar{I}}^r$ are the platform and rotor inertia dyadics, respectively, referred to the system center of mass.

$$\vec{\omega}_p = \dot{\theta}\hat{e}_1 + \dot{\psi}\hat{e}_{z_i} + \dot{\beta}_p\hat{e}_z \tag{5}$$

$$\vec{\omega}_r = \dot{\theta}e_1 + \dot{\psi}\hat{e}_{z_i} + \dot{\beta}_r\hat{e}_z \tag{6}$$

are the inertial angular velocities of the two bodies in terms of the rotations defined previously. The cone angle θ is defined by the distribution of angular momentum between the transverse axis and the normal spin axis.

$$\theta = \tan^{-1}\left[\frac{\vec{H}\cdot\hat{e}_2}{\vec{H}\cdot\hat{e}_3}\right] \tag{7}$$

$$I_{xx} = A + \Delta I_p + \Delta I_r \cos^2\emptyset \tag{8}$$

$$I_{yy} = A + \Delta I_r \sin^2\emptyset \tag{9}$$

are the transverse inertias, with A containing all constant terms common to I_{xx} and I_{yy} from both bodies.

Two inertia ratios of interest in the sequel are the ratio of bearing axis moments of inertia

$$J = B/C \tag{10}$$

and the roll/pitch ratio.

$$\sigma = C/A \tag{11}$$

B is the bearing axis moment of inertia of the platform, and C is that of the rotor. The inertial free precession frequency is given by

$$\lambda_0 = |\bar{H}|/A = C\omega_{ro}/A = \sigma\omega_{ro} \tag{12}$$

since the system angular momentum $|\bar{H}|$ is established by rotor inertia and the nominal spin speed with $\theta = \omega_p = 0$.

It is well known[11-13] that stabilization of a dual-spin spacecraft having energy dissipation on both bodies requires that

$$\dot{E}_p/\lambda_p + \dot{E}_r/\lambda_r < 0 \tag{13}$$

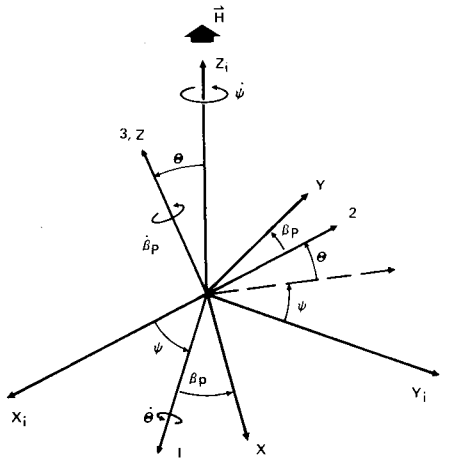

Fig. 2 Inertial coordinates.

where $\dot{E}_p$ and $\dot{E}_r$ are negative terms representing energy dissipation, and λ_p and λ_r are the frequencies of nutation as viewed in each body. For $\sigma > 1$, both λ_p and λ_r are greater than zero, so Eq. (13) is satisfied for any combination of $\dot{E}_p$ and $\dot{E}_r$. For $\sigma < 1$, $\lambda_r = \lambda_0 - \omega_r < 0$ and $\dot{E}_r/\lambda_r > 0$, so that

$$|\dot{E}_p| > |\sigma/(\sigma - 1)|\,|\dot{E}_r| \tag{14}$$

is a required condition to obtain nutational stability according to Eq. (13). $\dot{E}_r$ is primarily due to fuel slosh, and $\dot{E}_p$ is provided by a nutation damper and/or active coupling with the despin control system through a platform crossproduct of inertia such as shown in Fig. 1.

When the platform is spinning, however, the energy dissipation characteristics are modified. For small platform rates, the net damping characteristics are altered due to detuning of the nutation damper and/or crossproduct coupling and to varying the fuel slosh excitation frequency. For larger deviations from nominal operating conditions, various nonlinearities may appear such as saturation of the damper and torque motor, and different modes of fuel slosh behavior. For dual-spin vehicles having the specified kinds of mass asymmetry, however, the dynamic response with the platform rotating is dominated by interactions arising from bearing axis torque (an energy source or sink) acting on the rigid body properties of the vehicle.

Platform Spinup: $\sigma < 1$

As the unbalanced platform starts to rotate, a body-fixed torque due to the platform crossproduct generates a coning motion of the bearing axis at platform spin rate. The cone angle is determined by the distribution of angular momentum according to Eq. (7). In terms of the vehicle inertias and spin rates, the cone angle may be expressed as

$$\theta = \frac{I_{cp}}{C(\omega_r/\omega_p) + B - I_{xx}} \tag{15}$$

As a first step in investigating the vehicle interactions during platform spinup, consider the momentum distribution along the bearing axis, assuming small θ:

$$|\bar{H}| = C\omega_r + B\omega_p \tag{16}$$

Rearranging Eq. (16) to obtain platform rate as a function of rotor rate and normalizing both to the nominal rotor rate,

$$\omega_p/\omega_{ro} = (I/J)\,(1 - \omega_r/\omega_{ro}) \tag{17}$$

Figure 3 shows (for TACSAT parameters) the variation in body rates along the bearing axis from a despun platform

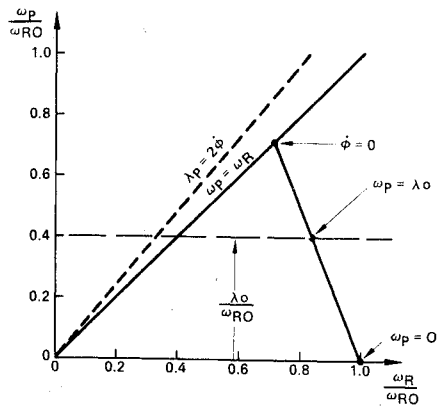

Fig. 3 Platform rate vs rotor rate during platform spinup for TACSAT parameters $\sigma = 0.4$, $J = 0.4$.

condition ($\omega_p = 0$) to the limiting condition of zero relative rate ($\omega_p = \omega_r$). The nominal operating point is at $\omega_p = 0$, $\omega_r = \omega_{ro}$. If the platform spins up due to bearing friction, platform rate and rotor rate vary along the indicated trajectory. Platform spinup due to friction stops when the relative rate goes to zero ($\dot{\varnothing} = 0$).

The normalized inertial free precession rate is shown in Fig. 3 as the long dashed line. The short dashed line describes a condition pertinent to nutation resonance, discussed herein. If $\sigma < 1$, the inertial free precession rate is less than the initial rotor spin rate (i.e., $\lambda_0 < \omega_{ro}$); if

$$\sigma < I/(I+J) \tag{18}$$

then platform rate will reach λ_0 during spinup. Simulation of platform spinup for the TACSAT vehicle provides an illustration of the dynamic interaction that can arise when Eq. (18) is satisfied. The inertias for TACSAT are as follows:

$$A = 970 \text{ slug-ft}^2$$
$$B = 159 \text{ slug-ft}^2$$
$$C = 400 \text{ slug-ft}^2$$
$$\Delta I_p = 12 \text{ slug-ft}^2$$
$$\Delta I_r = 5 \text{ slug-ft}^2$$
$$I_{cp} = -55 \text{ slug-ft}^2$$
$$\sigma = 0.4$$
$$J = 0.4$$

Figure 4 shows the body rates and cone angle time history during platform spinup due to friction. Initially, the cone angle increases with increasing ω_p according to Eq. (15), and ω_r decreases due to conservation of angular momentum along the bearing axis. At $t = 475$ s, however, the platform rate reverses and rotor momentum is transferred instead into a transverse axis, causing a more rapid growth in cone angle to its final value of 83 deg. At the end, the vehicle is in a state of pure spin about the maximum principle axis, with zero relative rate between the two bodies. The oscillation at $t = 1800$ s is a weak nutation resonance, discussed herein.

At $t = 475$ s, the platform rate is approximately equal to the inertial free precession frequency. Prior to that time, body-fixed torque due to the rotating platform mass asymmetries is varying slowly at platform spin rate. As the platform reaches λ_0, however, the net centrifugal force acting on the platform becomes synchronized with the inertial free precession (Fig. 5). In this condition, the net centrifugal force on the platform unbalance masses tends to maintain the indicated platform rotational position about the bearing axis. The friction spinup torque on the platform, however, is acting to accelerate the platform. If friction does not exceed the dynamic torque about the bearing axis, an equilibrium will be established. In the equilibrium, or phase-lock condition, the platform is fixed

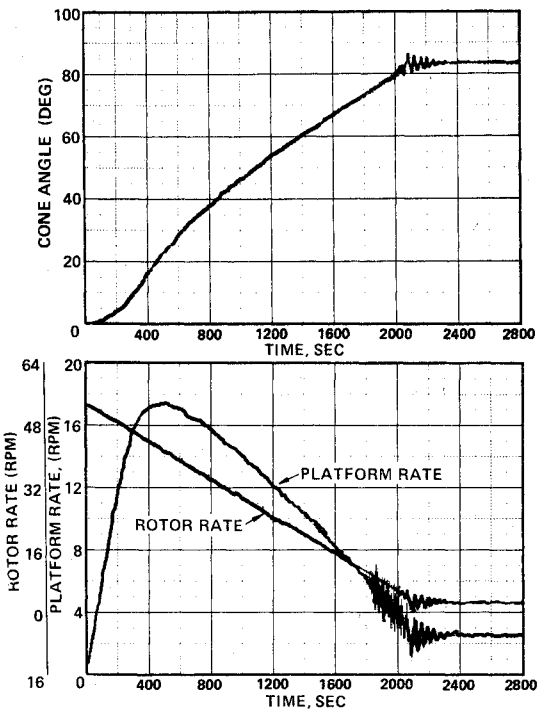

Fig. 4 Platform spinup for TACSAT mass properties.

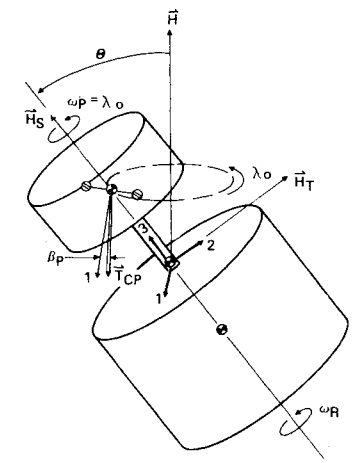

Fig. 5 Vehicle attitude in precession phase lock.

with respect to the momentum vector and rotated through an angle β_p that depends on the bearing friction.

Figure 6 depicts the resolution of the platform-fixed torque due to the crossproduct onto the inertial 1, 2, 3 coordinates. The effect of bearing friction on cone angle growth may be described by the projection of a component of the crossproduct torque onto the transverse angular velocity vector, which causes an increase in cone angle. Conservation of total momentum requires that spin axis momentum decrease, which is the effect of friction as it spins down the rotor. Without friction, the vehicle would remain in a state of equilibrium free precession, with a constant distribution of momentum between the spin and transverse axes.

If, on the other hand, the friction torque is large enough relative to the dynamic torques, the platform may continue to accelerate through the region of synchronism with the inertial free precession rate. In this case, the relative rate between the two bodies would go to zero at a relatively small cone angle. If the equivalent single body still had a roll/pitch ratio less than unity, the cone angle would gradually increase in the presence of other internal energy dissipation effects until the vehicle reached a state of pure spin about the maximum principal axis of inertia.

An approximate solution for the torque balance along the bearing axis can be obtained by taking the total time derivative of angular momentum in terms of inertial angles ψ, θ, and β_p, and assuming $\dot{\theta}=\dot{\beta}=\dot{\psi}=0$, corresponding to a captured condition. The component along the z axis is found to be

$$T_b^p=(\psi^2/2)\,[I_{cp}\sin\beta_p 2\theta+\Delta I_p \sin 2\beta_p \sin^2\theta] \qquad (19)$$

where T_b^p is the dynamic torque on the platform about the bearing axis due to platform asymmetries, and $\dot{\psi}=\lambda_0$. ΔI_p produces a maximum torque contribution at $\theta=90$ deg, $\beta_p=45$ deg, while torque due to I_{cp} is maximum at $\theta=45$ deg, $\beta_p=90$ deg. The platform azimuth angle β_p will change with θ, depending on the values of I_{cp}, and ΔI_p so as to satisfy Eq. (19). Equation (19) will be used below in determining the torque constraints for flat spin recovery by a reversal of the momentum transfer process just described.

Recovery from Flat Spin Condition: $\sigma<1$

Figure 7 illustrates the flat spin geometry for a vehicle having the asymmetry properties defined previously and a roll/pitch ratio $\sigma<1$. Both bodies reach an equilibrium attitude corresponding to their minimum energy state. The rotor, which is assumed to have transverse inertia asymmetry only, will assume the attitude indicated ± 180 deg. That is, the rotor asymmetry masses lie in a plane normal to the momentum vector. Any rotation of either body along the bearing axis represents an increased energy level and leads to centrifugal restoring forces arising from the rotation rate in flat spin λ_0.

The recovery process requires that the rotor be rotated out of its minimum energy condition. Equation (19), with a change of notation and without the I_{cp} term, gives the dynamic torque acting to maintain the rotor minimum energy attitude:

$$T_b^r=(\lambda_0^2/2)\,[\Delta I_r \sin 2\beta_r \sin^2\theta] \qquad (20)$$

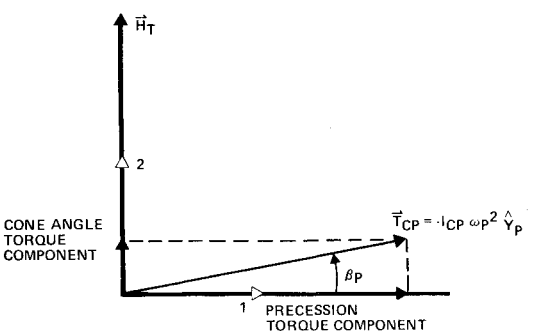

Fig. 6 Components of crossproduct torque.

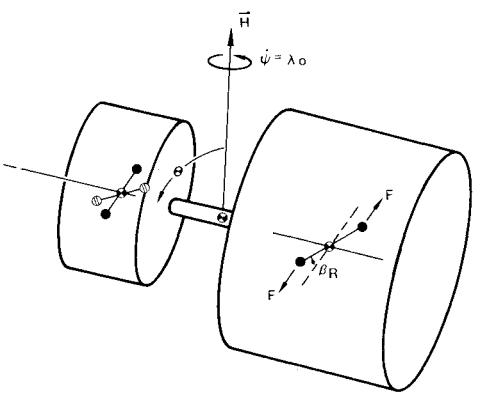

Fig. 7 Vehicle attitude in flat spin ($\sigma<1$).

Once the rotor has reached its equilibrium state, this dynamic torque due to transverse inertia asymmetry must be overcome before the divergence mechanism can be reversed to effect a recovery using the despin motor. Once the rotor has been rotated through 90 deg, however, the despin motor need only supply the average torque per rotation cycle i.e., friction plus other losses.

In order for recovery with the motor to proceed, the motor torque must be less than the dynamic torques due to platform asymmetry; otherwise, the applied torque would only counterrotate the two bodies, without the desired cone angle reduction by momentum transfer. As cone angle decreases in a successful recovery, the platform dynamic torques decrease as indicated by the form of Eq. (18). If the value of θ for which the motor torque exceeds the dynamic torque is small, the normal small angle stabilization system can complete the convergence to zero cone angle.

Figure 8 illustrates the various torque boundaries for flat spin recovery for an idealized set of mass properties. For the inertia asymmetry parameters selected to illustrate the concepts, the dynamic torque on the platform is much greater than the motor torque; also, the motor torque is somewhat larger than the peak dynamic torque on the rotor in flat spin (i.e., with $\beta_r=45$ deg in Eq. (20). Application of motor torque in this case will accelerate the rotor without counterrotating the platform. The transfer of momentum from the transverse axis to the spin axis will proceed as long as the applied torque can supply losses due to bearing friction, fuel slosh, etc. When the cone angle reaches 5-deg, the motor torque exceeds the platform dynamic torque. Final acquisition then requires damping of a 5 deg residual nutation angle and normal despin control of the payload platform.

In actual practice, motor torque may not be sufficient to overcome the peak dynamic torque on the rotor. Motor size is determined by bearing friction and normal despin acquisition requirements, which generally require smaller peak torque than flat spin recovery. Also, the rotor asymmetry cannot be precisely controlled and actually increases in flat spin due to redistribution of liquid propellant in the rotor. Some other means of initiating the recovery process may therefore be required. Two approaches are available: First, by applying motor torque in a pulse mode synchronous with rotor oscillation about the bearing axis, the rotor can be rotated if the available torque is sufficient to overcome the energy losses per cycle. Second, a timed firing of a spinup jet (if available) can provide additional torque to assist the despin motor in initially rotating the rotor.

Platform Spinup: $\sigma>1$

An oblate inertia distribution ($\sigma>1$) presents a related but quite distinct situation as regards platform spinup compared

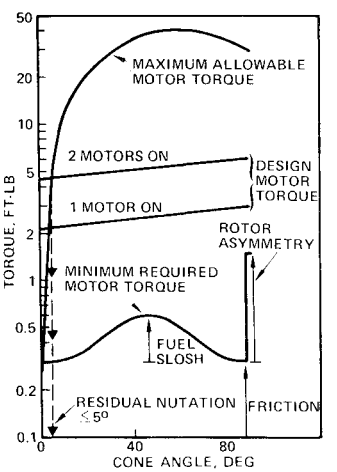

Fig. 8 Torque boundaries for flat spin recovery.

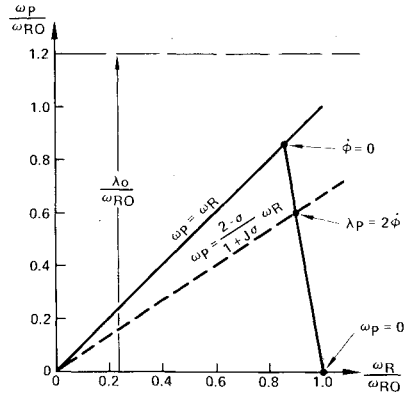

Fig. 9 Platform rate vs rotor rate during platform spinup for DSCS-II parameters $\sigma = 1.2$, $J = 0.7$.

to that for $\sigma < 1$. The same types of platform and rotor mass asymmetry affect the vehicle dynamics, but in a different way and with somewhat different implications for system design.

During the initial stage of platform spinup for $\sigma > 1$, the same type of coning motion of the bearing axis occurs as for $\sigma < 1$. The bearing axis cones at platform spin rate with a cone angle given by Eq. (15). The particular phase-lock interaction described above does not occur, however, since the platform never reaches the inertial precession rate λ_0 with $\sigma > 1$ (Fig. 9). Nevertheless, a dynamic interaction leading to nutation buildup can occur during platform spinup, as described below.

Figure 10 shows a simulated platform spinup for a vehicle with inertia parameters similar to DSCS-II:

$$A = 250 \text{ slug-ft}^2$$
$$B = 50 \text{ slug-ft}^2$$
$$C = 300 \text{ slug-ft}^2$$
$$\Delta I_p = 10 \text{ slug-ft}^2$$
$$\Delta I_r = 20 \text{ slug-ft}^2$$
$$I_{cp} = 20 \text{ slug-ft}^2$$
$$\sigma = 1.2$$
$$J = 0.17$$

The time histories show a relatively smooth increase in cone angle with platform rate up to $t = 1000$ s, when an abrupt change occurs. Body rate and cone angle undergo relatively large oscillations before converging on the steady-state solution of spin about the major principal axis at $t = 1900$ s. Since the minimum energy state of the system is pure spin about the major principal axis (near the bearing axis in this case), a dissipative friction torque eventually must drive the system to that state. However, this does not preclude an intermediate energy state in which relatively large nutation is developed. The interaction illustrated in Fig. 10 is the nutation resonance, or resonance trap, discussed in Refs. 8 and 9.

The nutation growth is predominantly cyclic, as opposed to the secular buildup of cone angle in the phase-lock interaction discussed above for $\sigma < 1$. We will take as a starting point for an understanding of the resonance phenomenon the magnitude of the cone angle during the initial platform rotation in Eq. (15). Since I_{xx} varies at $2\dot{\theta}$, the cone angle θ will vary about a mean value. This nodding motion of the bearing axis due to rotor transverse inertia asymmetry is an angular rate about the inertial 1 axis (Fig. 2) which is fixed with respect to the platform Y axis during coning (Fig. 11). As long as the frequency of this induced angular velocity (i.e., $2\dot{\theta}$) is sufficiently separated from the platform nutation frequency λ_p, nutation induced by this disturbance tends to average to zero over many cycles. If the two frequencies are equal, however, the transverse rate due to rotor asymmetry contributes to a systematic buildup of nutation, as illustrated in Figs. 12a through 12f. The figures represent the angular velocities in the 1-2 plane of Fig. 2 during nutation resonance. At time t_0 (Fig. 12a), there is a transverse angular velocity $\omega_p \tan\theta$ associated with precession of the spinning unbalanced platform. The angular velocity induced by the rotor asymmetry torque in Fig. 12a is reflected in an increased transverse velocity in Fig. 12b. In Fig. 12c, the induced velocity has rotated 180 deg, and the opposite polarity of torque due to rotor asymmetry further increases the induced velocity. At each half-cycle of relative rotation, a systematic buildup of velocity $\dot{\theta}$ occurs and is reflected in an oscillatory growth in the cone angle since the transverse angular velocity buildup is at platform nutation frequency λ_p.

Substituting $\lambda_p = \lambda_0 - \omega_p$ in the necessary condition for resonance, $\lambda_p = 2\dot{\phi}$, the ratio of body spin rates at resonance is

$$\frac{\omega_p}{\omega_r} = \frac{2\cos\theta - \sigma}{\cos\theta + J\sigma} \tag{21}$$

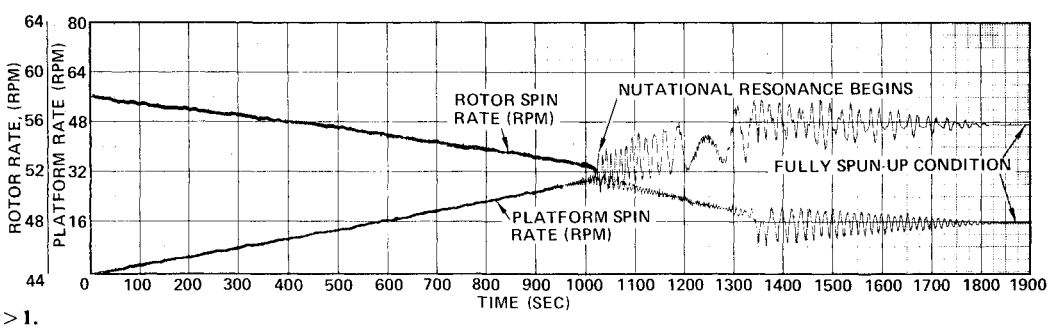

Fig. 10 Platform spinup for $\sigma > 1$.

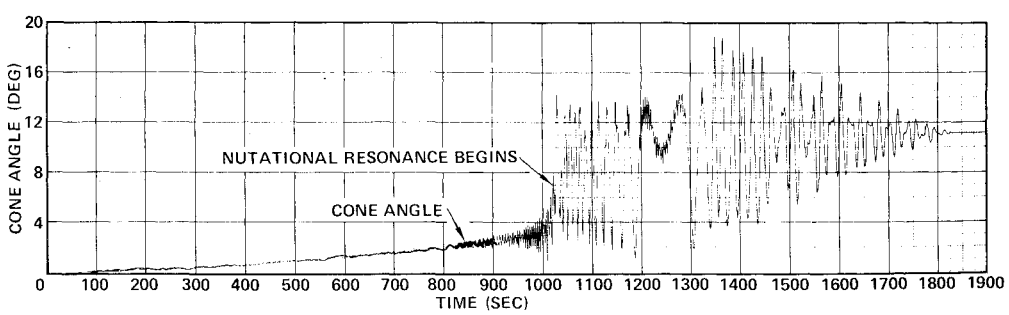

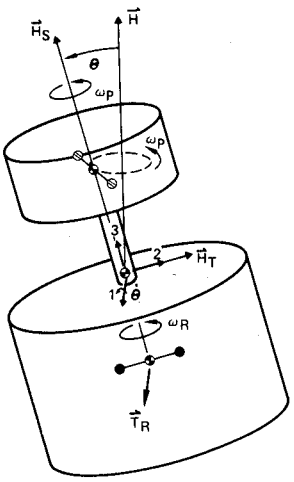

Fig. 11 Vehicle attitude in nutation resonance.

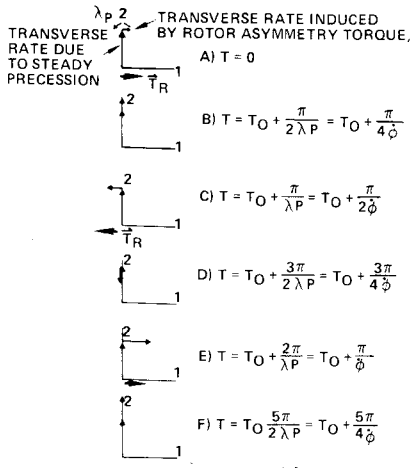

Fig. 12 Transverse rate buildup in nutation resonance.

For $\sigma > 1$, θ tends to be small, so that

$$\frac{\omega_p}{\omega_r} \approx \frac{2-\sigma}{1+J\sigma} \tag{22}$$

The short dashed line in Fig. 9 is a plot of Eq. (22). For $\sigma > 1$, the slope of this line is less than unity, so that $\lambda_p = 2\dot{\phi}$ for some platform rate below the limiting condition of zero relative rate.

$\lambda_p = 2\dot{\phi}$ is not a sufficient condition for nutation resonance since a platform crossproduct of inertia and rotor transverse inertia asymmetry are required to produce rotor-fixed driving torque. If the applied torque is not sufficient to escape the resonance region, the platform rate can be captured and the applied torque is then contributing to nutation buildup rather than to changing the platform rate. Determination of torque boundaries for capture in resonance is complicated by the time-varying nature of the problem. Simulation is the most straightforward current means of establishing bounds for motor torque and mass asymmetries in a particular case to ensure passage through resonance.

Finally, note that large θ, such as may occur for vehicles with $\sigma < 1$, leads to a modified relative rate condition for resonance Eq. (21). It is therefore possible for the condition $\lambda_p = 2\dot{\phi}$ to be met at a large cone angle during flat spin divergence of a vehicle with $\sigma < 1$. This is the case for the TACSAT flat spin simulation shown in Fig. 4. Since the system is near its minimum energy, a nutation resonance in this parameter regime tends to be relatively weak.

Recovery from All-Spun Condition: $\sigma > 1$

The same set of dynamic torques acts on the two bodies for $\sigma > 1$ as in the case of flat spin recovery with $\sigma < 1$, but the equilibrium cone angle θ is smaller. θ is given by Eq. (15) with $\omega_r/\omega_p = 1$. The spin rate in this case is

$$\dot{\psi} \approx C_{\omega_{ro}}/(C+B) = \omega_{ro}/(I+J) \tag{23}$$

The principal considerations for recovery are initiating relative motion and passing through the regime of the nutation resonance. Since the recovery nominally proceeds by a simple exchange of momentum along the bearing axis, there is not an upper bound on the applied torque as for $\sigma < 1$. Motor pulsing may be required to overcome the dynamic torques, establishing relative motion, or continuous motor torque will establish relative motion if the available torque exceeds that given by Eqs. (19) and (20).

During platform despin, the nutation resonance region will again be encountered. In this case, the net bearing axis torque due to the despin motor is an energy source and can therefore produce a larger nutation buildup than during the spinup resonance encounter.[8] The specified mass asymmetries and despin motor torque capability must therefore be matched such that the platform can be despun from the all-spun condition (zero relative rate) without a significant nutation buildup. Once the platform inertial rate is nulled, any residual nutation will be damped by internal losses since $\sigma > 1$ [Eq. (13)].

On-Orbit Experience

DSCS-II and TACSAT are dual-spin satellites having the types of mass asymmetries considered here. DSCS-II encountered dynamic interaction difficulties with the first flight vehicles, resulting in modifications to subsequent spacecraft to ensure a well-behaved platform spinup. TACSAT diverged to flat spin due to motor brush failure after having exceeded its design life by nearly a year. Recovery operations were carried out for both vehicles, as described below.

The first pair of DSCS-II satellites was launched in 1971. Spinup of the payload platform occurred later that year on one of those vehicles due to an apparent electronic malfunction. When the alternate electronic unit was commanded to despin the platform, the motor was not able to initiate relative motion. Subsequent analysis and simulation studies revealed the dynamic interactions associated with a platform crossproduct of inertia and rotor transverse asymmetry.

Initial recovery attempts utilized open-loop pulsing of the motor to overcome the dynamic torques, which were approximately 10 times the available motor torque. Large amplitude relative motion was obtained by adjusting the period of motor torquing, but the amplitude was not sufficient to initiate the desired buildup of relative rates.

Before further orbital tests, however, a more comprehensive simulation model demonstrated the nutation resonance phenomenon for the first time. The complex, time-varying equations of motion made a general analysis and solution impractical; therefore, a control law was sought by continued use of simulations. The resonance condition proved to be an even more difficult challenge than initiating relative motion from the all-spun condition. Control laws for motor torque were eventually discovered, however; closed-loop on-off control of the motor using simulated received antenna signal strength as feedback was effective for initiating relative motion and despinning through resonance to a despun platform state.

When the new control laws were tried on the flight spacecraft, however, energy dissipation effects as yet unmodeled precluded buildup of a large enough relative angle to initiate the despin. This discovery led to utilization of the available jets (axial and radial) to develop the larger control torques needed to overcome internal energy dissipation.

Again, a suitable control law was developed that used real-time feedback information and required precise timing of commands. This time the orbital operations were successful and the vehicle was restored to normal operation in June, 1972.

Subsequent flight spacecraft have been modified to ensure platform recovery from the all-spun condition. A balance weight was added to the despun platform to substantially reduce the crossproduct of inertia, and the propellant tanks were reconfigured to make the rotor transverse inertias nearly equal.

TACSAT was launched in 1969 and operated until late 1972, exceeding its design life by nearly a full year.[14] The despin motor used wet lubricated brushes for commutation. In late 1972, intermittent motor current indicated a probable degradation in the brush condition. As the delivered average motor torque decreased below bearing friction, the platform spun up. Divergence to flat spin occurred as described above for $\sigma < 1$.

Once in the flat spin condition, with no relative motion in the bearing assumbly, telemetry of motor current indicated a constant maximum value. In the absence of relative motion, the motor brushes were apparently conducting normally, but the vehicle remained in flat spin since the delivered torque was below that required to overcome the dynamic torques. It was decided to attempt a recovery on the possibility that migration of oil in the despin assembly might have rejuvenated the motor brushes to a sufficient extent to support normal operation for some period of time.

Since flat spin recovery had not been a consideration in the design of TACSAT in 1967, the recovery attempt required considerable modification to the nominal recovery methods discussed above. The rotor was determined to be more asymmetric than the platform, making it very difficult to spin up the rotor without counterspinning the platform, as required for recovery. Furthermore, the spinup jets could not be utilized since they were designed for initial spinup only, using a simple blow-down system. The axial and radial jets could be commanded, however, and the despin motor could be controlled in an on-off mode. Feedback information for real-time control was provided by modulated signal strength from a toroidal beam telemetry/command antenna and from a directional beacon.

In order to develop a recovery strategy using the limited feedback and control torques, a real-time simulation of the vehicle dynamics and telemetry signals was developed. By commanding the actual spacecraft motor torque on and off using the simulation, a comparison was made of the simulated and actual response. Once a reasonable correlation was obtained over a range of excitation frequency, indicating a matching of the critical mass properties parameters, experiments were conducted using the simulation to determine a control torque sequence to initiate the recovery. The recovery sequence developed with the aid of the simulation had three parts: first, platform oscillation was built up using the despin motor in a pulse mode; second, motor torque was left on and the platform was allowed to make a complete revolution about the bearing axis causing the rotor displacement to increase; and third, an axial and a radial jet were fired to reduce the net torque on the platform, trapping it in oscillation about the momentum vector while the rotor continued to spin up under the influence of motor torque. The recovery attempt was made in June of 1973. When the planned control torque sequence was successfully executed, the vehicle response closely parallelled that of the simulation. The antenna patterns confirmed that the intended reduction in cone angle had indeed occurred, but telemetry of motor current and brush temperature showed that the motor brushes had not be substantially rejuvenated by oil migrated in flat spin. Delivered torque began to decrease once again, as brush contact became increasingly erratic, and the vehicle returned to a flat spin condition after reaching a minimum cone angle of approximately 30 deg.

Conclusions

The theoretical and practical experience gained from the DSCS-II and TACSAT recovery operations, combined with related studies in industry and elsewhere, has provided valuable insight into dynamic interactions that may occur if the payload platform of a dual-spin satellite spins up. The interactions arise from platform dynamic imbalance and transverse inertia asymmetry, and from rotor transverse inertia asymmetry. Since such asymmetries must often be accepted as part of a realistic system design, consideration of platform spinup dynamics is a key part of the design process for current and future vehicles of this type. Somewhat different considerations apply, however, depending on the roll/pitch ratio.

For $\sigma > 1$, it is generally desirable to minimize platform dynamic imbalance and rotor transverse asymmetry in order to ensure recovery from the all-spun condition and passage through the nutation resonance region with a despin torque motor sized primarily for overcoming normal running friction. Once these conditions are satisfied, platform spinup to zero relative rate can constitute a low-power standby mode of operation for the spacecraft.

For $\sigma < 1$, an asymmetric and/or unbalanced platform and a symmetric rotor are preferred. Platform unbalance, combined with appropriate despin control system design, provides increased nutational stability margin. Platform unbalance and transverse inertia asymmetry also aid in recovery from flat spin by internal momentum transfer using the despin motor. In order to minimize the probability of flat spin for $\sigma < 1$, switchover to a redundant control system is made in the event of loss of platform despin control. The switchover is either an automatic onboard function or a ground-commanded operational procedure, depending on the mission requirements.

In addition to vehicle mass properties management and failure mode logic, some control system design features for normal operation are also pertinent to recovering from a flat spin or all-spun condition. Reuseable spinup jets utilized for infrequent spin trim maneuvers over the mission provide a means of rotating the rotor from its minimum energy attitude so that a reasonable amount of rotor transverse inertia asymmetry is allowable without requiring an oversized despin motor. Active nutation control using an axial jet controlled by an onboard accelerometer, in combination with the spinup jets, provides a means of controlling the distribution of angular momentum in body coordinates using external torques. A combination of internal momentum transfer using the despin motor and redistribution of angular momentum in body coordinates by jet torques provides several alternative recovery procedures in the unlikely event of an operational satellite going into a flat spin condition.

Considered early in the design phase, the large-angle dynamics of a dual-spin satellite can be accommodated in a straightforward manner. The simplicity and reliability of dual-spin stabilization is further enhanced by a basic understanding of large-angle dynamics and the requirements for recovery to a normal operating condition.

Acknowledgments

The author would like to thank M.W. Haupt of Hughes Aircraft Company for his suggestions regarding a heuristic description of nutation resonance and for simulation results used in the paper. Appreciation is also given to the DSCS-II Program Office of SAMSO and to TRW Systems Group for their assistance and cooperation.

References

[1] Velman, J.R. and Belardi, J.W., "Gyrostat Attitude Dynamcics," Hughes Aircraft Company, Los Angeles, Calif., SSD 90159R, May 1969.

[2] Adams, G.J., "Analog Simulation of the Dynamics and Control of Dual Spin Satellites," *Proceedings of the 1970 Summer Computer Simulation Conference*, Boston, Mass.

[3] Barba, P.M., Furumoto, N., and Leliakov, I.P., "Techniques for Flat Spin Recovery of Spinning Satellites," AIAA Paper No. 73-859.

[4] Kluiters, M., "Flat Spin Recovery of a Spinning Satellite," AIAA Paper No. 76-1946.

[5] Gebman, J.R. and Mingori, D.L., "Perturbation Solution for the Flat Spin Recovery of a Dual-Spin Spacecraft," AAS Paper 75-044.

[6] Barba, P.M. and Auburn, J.N., "Satellite Attitude Acquisition by Momentum Transfer," AAS Paper 75-043.

[7] Kaplan, M.H. and Patterson, T.C., "Attitude Maneuver for Bias Momentum Satellite," *COMSAT Technical Review,* Vol. 6, No. 1, Spring 1976.

[8] Scher, M.P. and Farrenkopf, R.L., "Dynamic Trap States of Dual Spin Spacecraft," AIAA Paper 73-908.

[9] Cochran, J.E., "Nonlinear Resonance in the Attitude Motion of a Dual-Spin Spacecraft," AIAA Paper No. 76-787.

[10] "TACSAT Final Report," Hughes Aircraft Company, SCG 30338R, Sept. 1973.

[11] Iorillo, A.J., "Nutation Damping Dynamics of Axisymmetric Rotor Stabilized Satellites," *Proceedings of the ASME Annual Winter Meetings,* Chicago, Ill., Nov. 1965.

[12] Likins, P.W., "Attitude Stability Criteria for Dual-Spin Spacecraft," *Journal of Spacecraft and Rockets,* Vol. 4, Dec. 1967, pp. 1638-1643.

[13] Neer, J.T., "Intelsat IV Nutation Dynamics," AIAA Paper No. 72-537.

[14] Brandes, R.D., "The Tactical Communications Satellite," *IEEE Transactions on Aerospace and Electronic Systems,* Vol. AES-6, No. 4, July 1970